frontiers | Frontiers in Earth Science

TYPE Original Research
PUBLISHED 16 September 2022
DOI 10.3389/feart.2022.992842

OPEN ACCESS

EDITED BY
Biswajeet Pradhan,
University of Technology Sydney, Australia

REVIEWED BY
Supattra Puttinaovarat,
Prince of Songkla University, Thailand
Paramate Horkaew,
Suranaree University of Technology, Thailand

*CORRESPONDENCE
Jianrong Fan,
fjrong@imde.ac.cn

†These authors have contributed equally to this work

SPECIALTY SECTION
This article was submitted to Geohazards and Georisks, a section of the journal Frontiers in Earth Science

RECEIVED 13 July 2022
ACCEPTED 23 August 2022
PUBLISHED 16 September 2022

CITATION
Fan J, Xu F, Zhang X, Zhang X and Liang B (2022), Evaluating the sensitivity and influential factors of freeze-thaw erosion in Tibet, China.
Front. Earth Sci. 10:992842.
doi: 10.3389/feart.2022.992842

Evaluating the sensitivity and influential factors of freeze-thaw erosion in Tibet, China

Jianrong Fan[1*†], Fubao Xu[1,2†], Xiyu Zhang[1], Xiaoxue Zhang[3] and Bo Liang[3]

[1]Research Center for Digital Mountain and Remote Sensing Application, Institute of Mountain Hazards and Environment, Chinese Academy of Sciences, Chengdu, China, [2]University of Chinese Academy of Sciences, Beijing, China, [3]Soil and Water Conservation Bureau of Tibet Autonomous Region, Lhasa, China

Freeze–thaw (FT) erosion has gradually become more severe due to climate warming, and concerns about FT erosion in ecologically fragile areas (e.g., high-altitude and high-latitude areas) continues to grow. Tibet, located at the Third Pole of Earth, is also in a substantial part underlain with seasonally frozen soil and subject to FT erosion. Evaluating the sensitivity and influential factors of FT erosion in Tibet is warranted to manage the ecological environment and human production activities. In this study, we investigated the sensitivity and spatial distribution characteristics of FT erosion in Tibet based on advanced remote sensing and geographic information system (GIS) technologies. To further explore the influence of each factor on FT erosion, we analyzed the sensitivity of FT erosion under each factor condition. Our results showed that the annual temperature range is the most influential factor on FT erosion among temperature, precipitation, topography and vegetation. In addition, we introduced the coefficient of variation (CV) to represent the stability of temperature and then used CMIP5 simulation data to estimate the susceptibility of FT erosion in Tibet over the next 30 years. The CVs in central and western Tibet were higher than those in other areas and thus need more attention to FT erosion in central and western Tibet in the future.

KEYWORDS

FT erosion, sensitivity assessment, GIS, remote sensing, Tibet

Introduction

Freeze-thaw caused by frequent changes of temperature is one of the most crucial characteristics of the land surface in high latitudes, which leads to the change of water volume in soil parent material pores or rock cracks (Gao et al., 2018). One of the serious hazards caused by Freeze-thaw changes is Freeze-thaw erosion. Freeze-thaw (FT) erosion refers to soil erosion resulting from FT alteration in slopes, trench walls, riverbeds, and canals in permafrost (Zhang et al., 2007; Hu et al., 2019). It mostly occurs at high latitudes and altitudes during late winter and early spring periods. It directly affects the hydrological process of frozen soil, changes soil water conductivity and soil water capacity, and threatens vegetation growth (Dong et al., 2000; Li et al., 2015). In

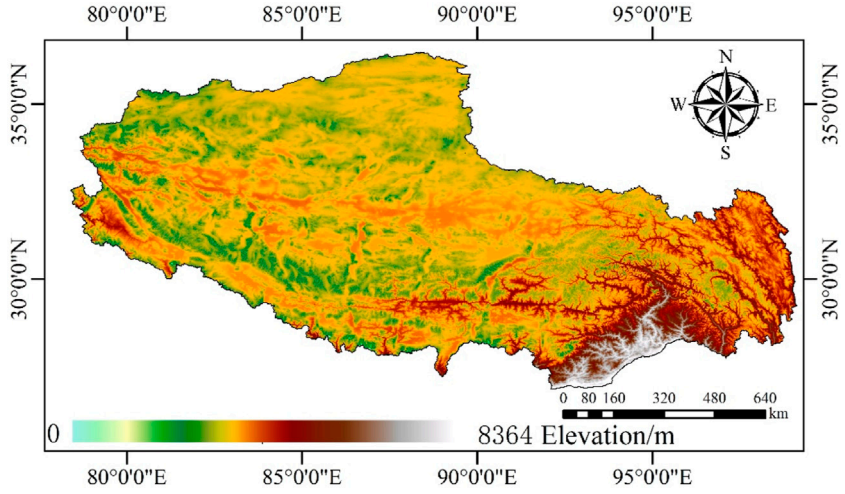

FIGURE 1
Map of study area.

TABLE 1 Overview of the dataset used in this paper.

Dataset	Variables	Spatial resolution	Year	Temporal resolution
SRTM DEM	slope, aspect	30 m	—	—
TRMM	precipitation	0.25°	2016–2018	3 h
MOD13/MYD13	NDVI	250 m	2016–2018	16 days
CRU	surface temperature	0.5°	2016–2018	Daily
CMIP5	surface temperature	1.125o	2019–2,100	Monthly

TABLE 2 Sensitivity of the evaluation factors.

Evaluation factor	Sensitivity				
	Insensitive	Mild	Moderate	High	Extremely high
Annual range of temperature (°C)	≤18	18–20	20–22	22–24	>24
Annual precipitation (mm)	≤100	100–200	200–300	300–400	>400
Slope (°)	0–3	3–8	8–15	15–25	>25
Aspect (°)	0–45, 315–360	45–90, 270–315	90–135	225–270	135–225
Vegetation coverage (%)	≥80	60–80	40–60	20–40	<20
Grading assignment	1	3	5	7	9

addition, FT erosion has become the primary form of erosion in cold regions and therefore is a substantial threat to the environment. In recent years, global warming has exerted a significant impact on terrestrial ecosystems (Reichstein et al., 2013; Wang et al., 2020), and FT erosion processes have been exacerbated due to rising temperatures (Wang et al., 2020). The Intergovernmental Panel on Climate Change (IPCC) fifth assessment report shows that the global average temperature increased by 0.85°C between 1880 and 2012 (Field et al., 2014). Therefore, increased attention to the prevention and treatment of FT erosion is important (Guo et al., 2017). In China, the freeze-thaw erosion covers an area of 1,269,800 km^2, which accounts for

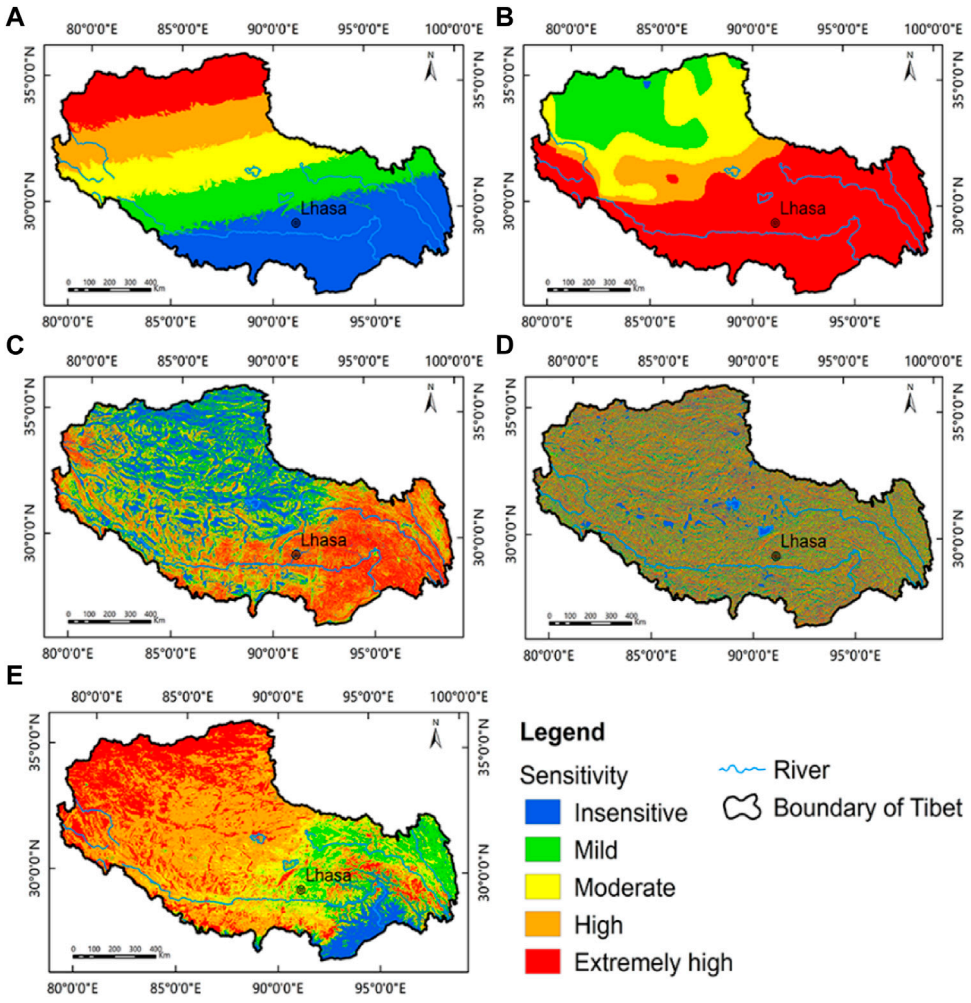

FIGURE 2
Spatial distributions of FT erosion sensitivity factors in Tibet: **(A)** annual temperature range, **(B)** annual precipitation, **(C)** slope, **(D)** aspect and **(E)** vegetation coverage.

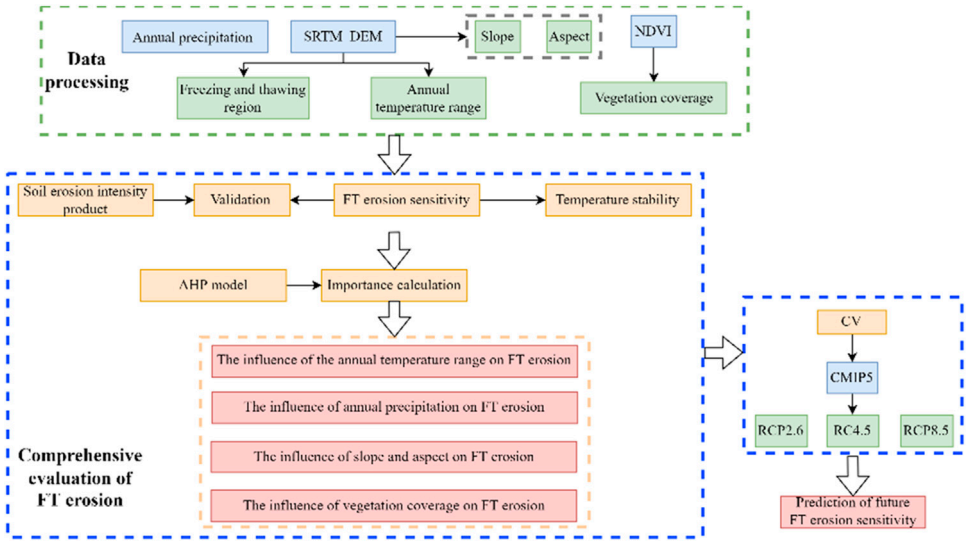

FIGURE 3
Flow chart of evaluating the FT erosion sensitivity in Tibet.

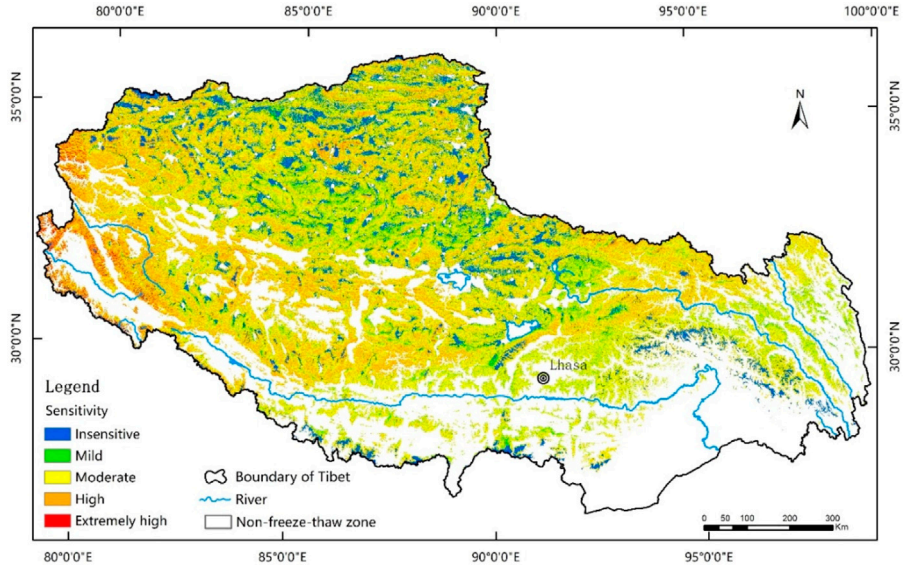

FIGURE 4
Sensitivity of FT erosion.

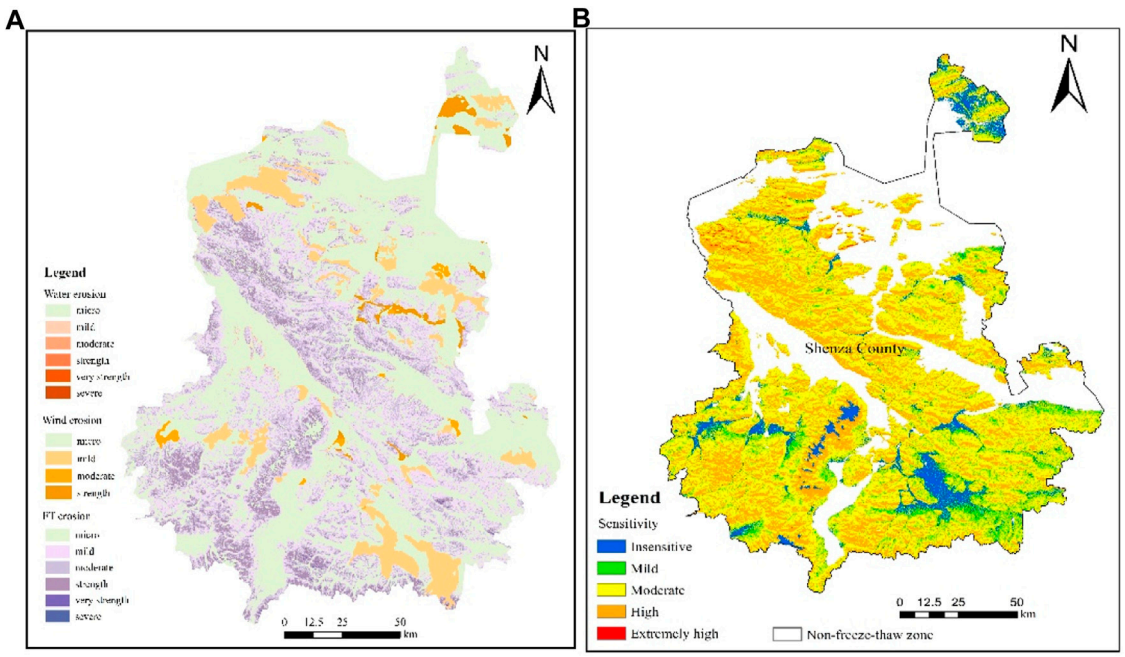

FIGURE 5
Comparison of FT erosion (Shenza County). **(A)** The result of soil erosion intensity product. **(B)** The result of FT erosion sensitivity.

13.36% of the total land area (Wei et al., 2012; Lu et al., 2021). Tibet appears to be particularly vulnerable to climate change and has become one of the most degraded ecosystems in the world (Teng et al., 2018). Moreover, FT erosion is widespread and has a great influence on engineering construction and agricultural activities in Tibet (Li et al., 2008; Zhang and Liu, 2018).

Sensitivity evaluation of FT erosion, particularly at the regional scale, could provide important insights into the prevention and treatment of FT erosion. However, FT erosion is affected by many factors, such as topography, precipitation, temperature, and vegetation, making its sensitivity complicated to evaluate. In recent years, numerous studies have focused on evaluating the sensitivity of soil erosion. Ferrick and Gatto. (2005) quantified FT erosion through laboratory experiments and demonstrated that FT is a primary process contributing to soil erosion in cold climates. Guo and Jiang. (2017) used eight typical factors to establish an evaluation method of FT erosion for the three-river source region in the Qinghai-Tibetan Plateau. Li et al. (2014) used a numerical moisture-heat-mechanics model to explore the FT damage mechanism. Eigenbrod (1996) obtained a linear relationship between the net volume changes after freezing and thawing. Lu et al. (2021) selected seven evaluation factors to analyze the temporal and spatial characteristics of freeze-

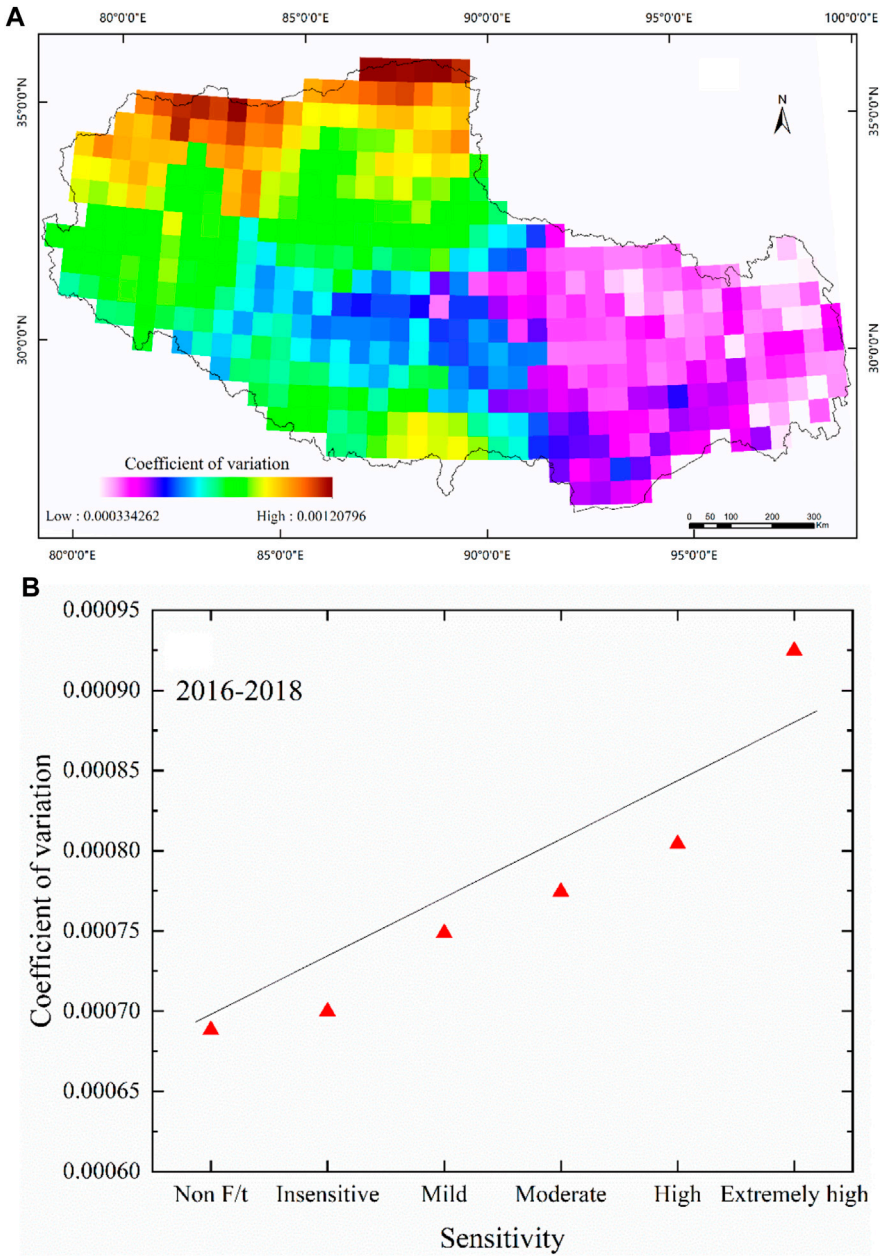

FIGURE 6
(A) Spatial distribution of CV from 2016 to 2018 in Tibet; **(B)** The mean CV in Tibet under different sensitivities.

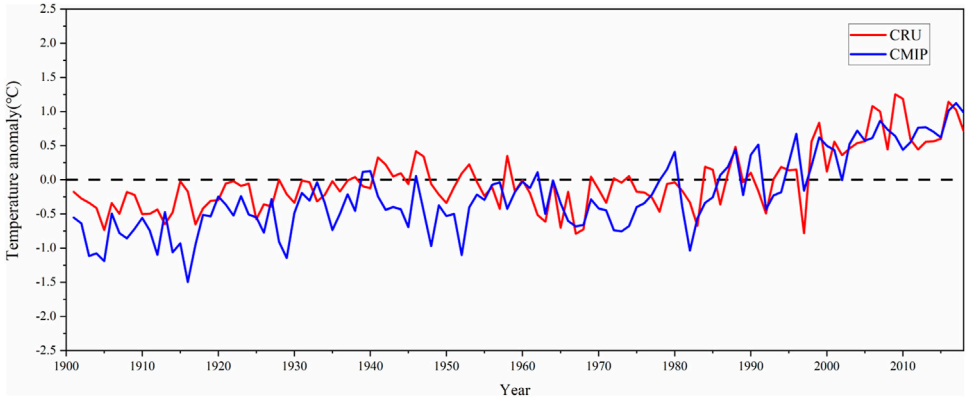

FIGURE 7
Time series of annual mean surface air temperature anomalies with respect to the 1981–2000 mean from CMIP5 and CRU during 1901–2018 over Tibet.

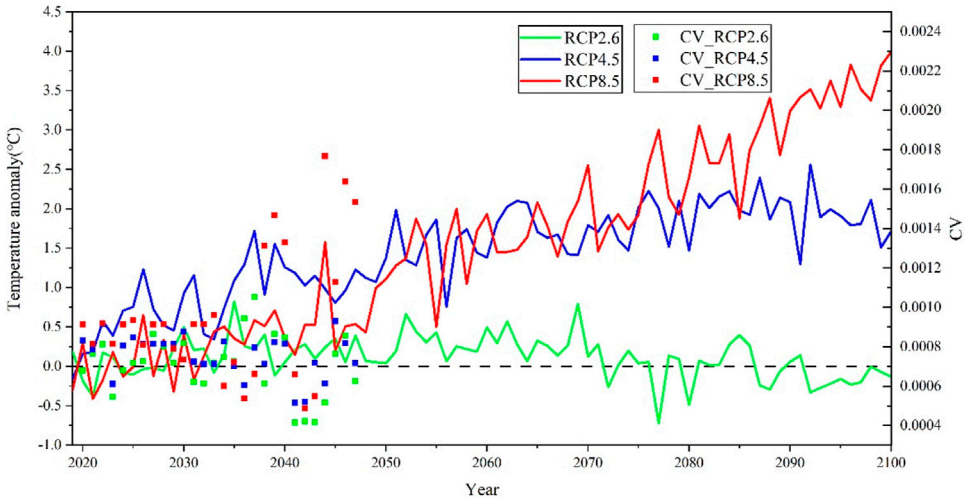

FIGURE 8
Temporal changes in annual mean surface air temperature anomalies with respect to 2019–2020 from different CMIP5 experiments during 2019–2,100 over Tibet.

thaw erosion in the source regions of the Chin-Sha, Ya-Lung and Lantsang Rivers. Guo et al. (2015) established an estimation model of FT erosion by introducing microwave remote sensing techniques. Shi et al. (2012) used the normalized method and evaluation model of freeze-thaw erosion with graded weight, the precipitation, annual temperature difference, vegetation index, slope and solar radiation to carry quantitative research and analysis in the three rivers source area. Additionally, many researchers have assessed the sensitivity of FT erosion and its impact on the environment (Liu et al., 2006; Zhang et al., 2007; Zhang et al., 2009; Kong and Yu, 2013; Liu et al., 2013).

FT erosion sensitivity is used to identify regions that are prone to freeze–thaw erosion and provide a scientific basis for human production and life (Wang et al., 2017). The objective of this study is to assess current FT erosion sensitivity levels in Tibet and evaluate the influence of different factors on FT erosion. Additionally, we evaluated the distribution of FT erosion probability with temperature from the CMIP5 model in the 21st century. In detail, we selected temperature, precipitation, slope, aspect and vegetation coverage as major factors to assess current FT erosion sensitivity based on a comprehensive analysis. The erosion intensity was classified as mild, moderate, high or extremely

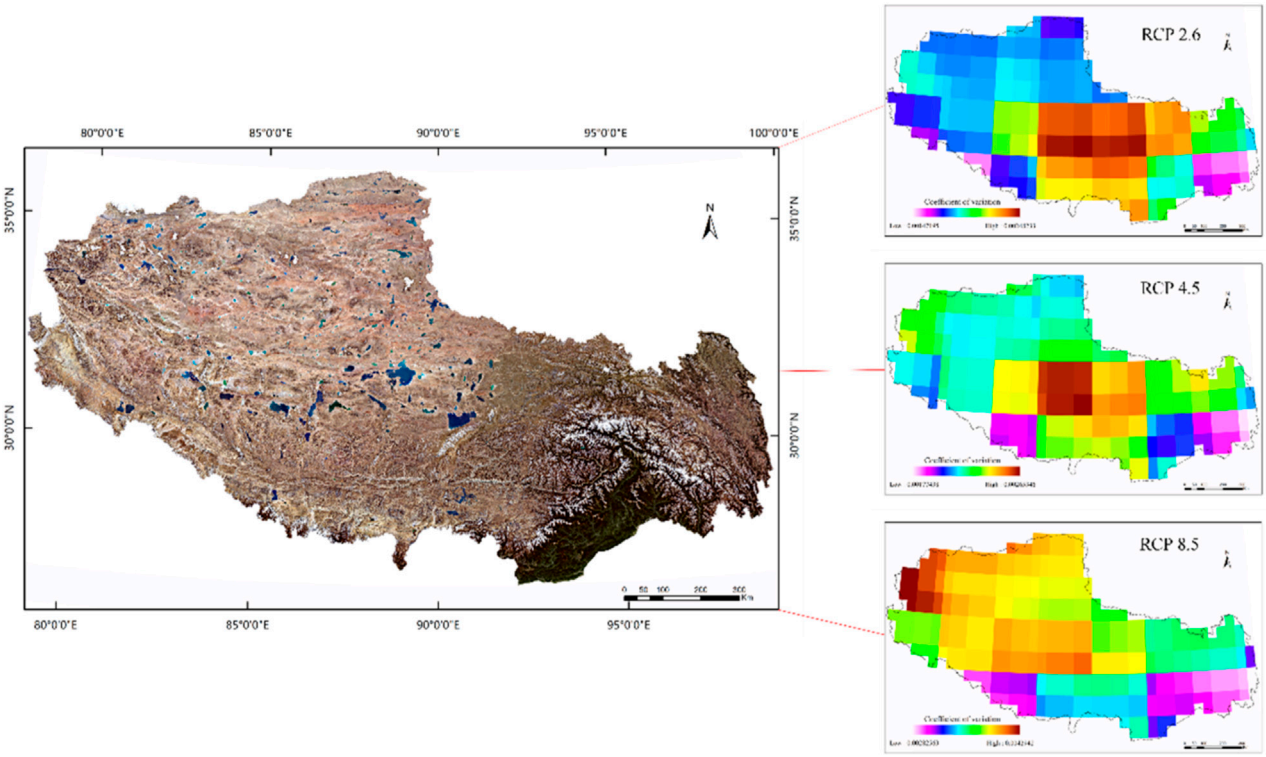

FIGURE 9
The distribution characteristics of CVs (RCP 2.6, RCP 4.5 and RCP 8.5 are displayed in the first, second and third rows on the right, respectively).

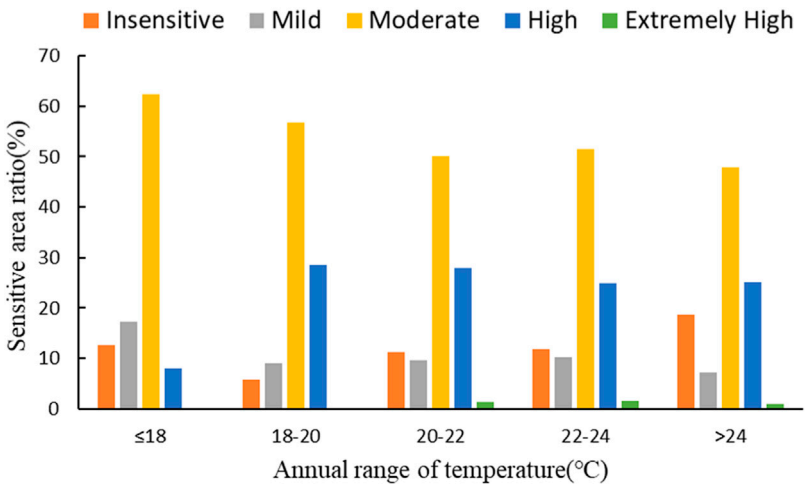

FIGURE 10
Ratios of different FT erosion sensitivities under various annual temperature ranges.

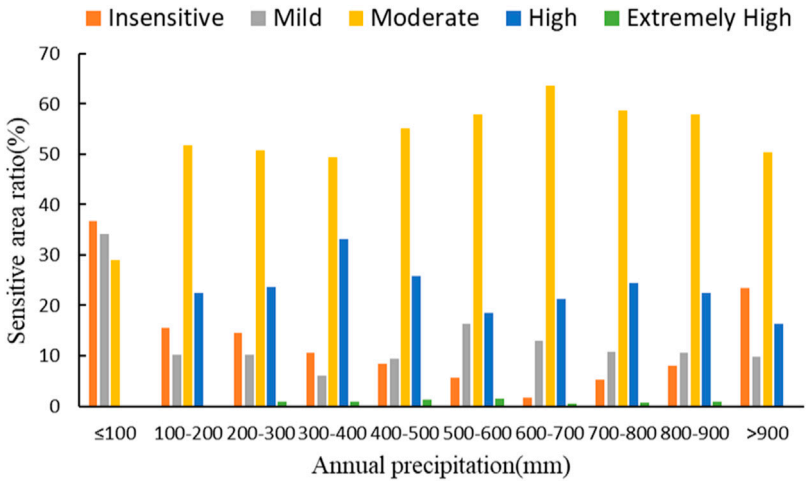

FIGURE 11
Ratios of different FT erosion sensitivities under various precipitation levels.

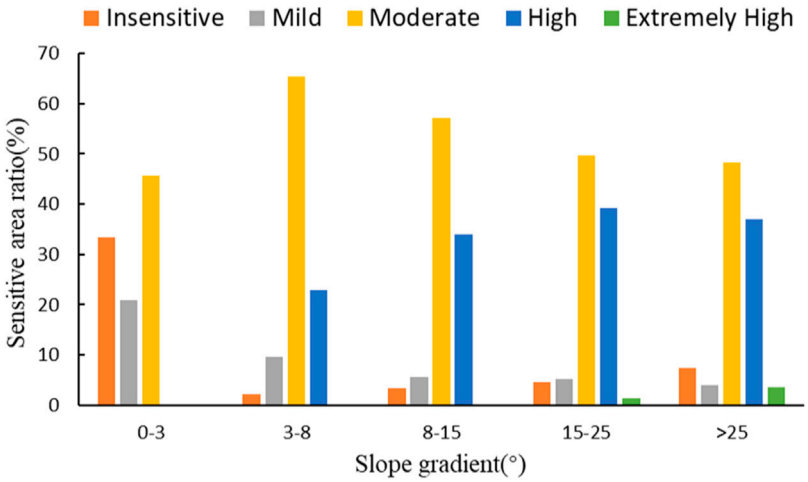

FIGURE 12
Ratios of different FT erosion sensitivities under various slope ranges.

high. Furthermore, we introduced the coefficient of variation (CV) to represent the future FT erosion probability.

Study area and materials

Study area

Tibet is located in Southwest China, spans between 26°50′-36°53′E and 78°25′-99°06′N, covers an area of 1,228,400 km^2 and belongs to an alpine subcontinent climate. It accounts for more than half of the Tibetan Plateau, and areas over 4,000 m above sea level account for 85.1% of the total area (Figure 1). The annual average temperature in Tibet is 4.2°C, and the average annual precipitation, which is mainly concentrated in summer, is 593.7 mm. The diverse soil types and the alternating FT cycles create conditions for the development of FT erosion. Tibet and its high mountainous regions are the most concentrated and intense regions of FT erosion in China (Li et al., 2005).

Data collection

The elevation data were provided by the NASA Shuttle Radar Topography Mission (SRTM) at a resolution of

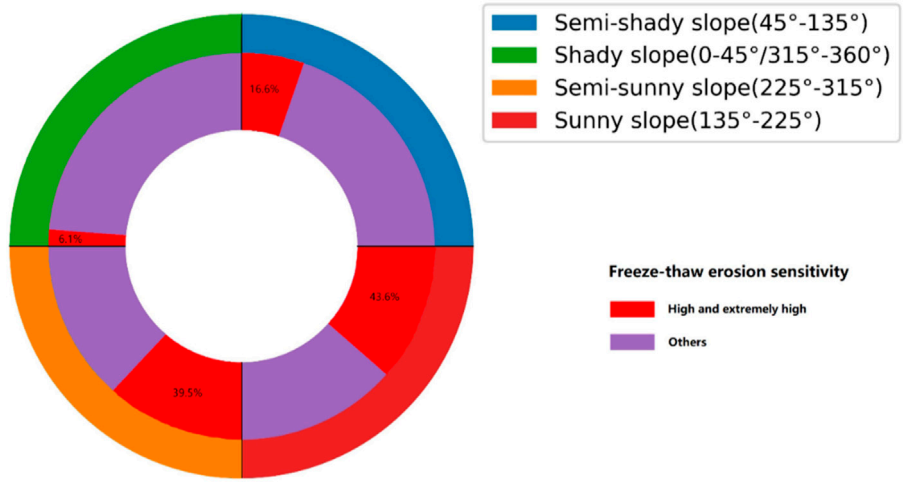

FIGURE 13
Ratios of different FT erosion sensitivities under various aspect ranges.

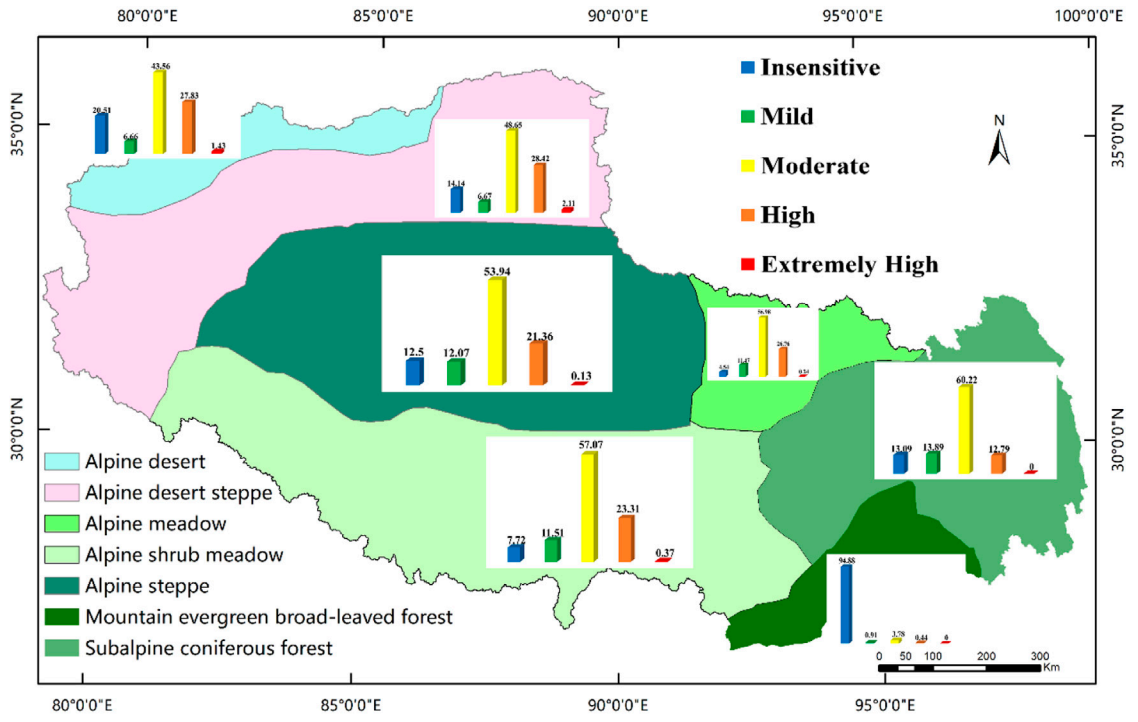

FIGURE 14
Vegetation distribution map and erosion ratios in Tibet.

approximately 30 m. The dataset has an absolute vertical accuracy of less than 16 m, and the relative vertical accuracy is less than 10 m (at the 90% confidence level) (Falorni et al., 2005). Slope and aspect were also derived based on the elevation, and the average pixel values were calculated to represent the surface morphology of the 90-m pixel.

TRMM precipitation data were provided by NASA (https://gpm.nasa.gov/data-access/downloads/trmm) (Huffman et al., 2010). The spatial resolution of the data was 0.25°, and the

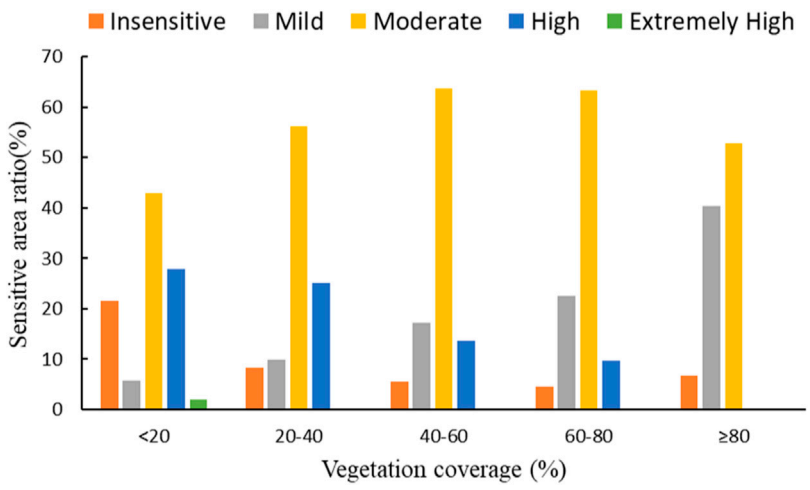

FIGURE 15
Ratios of different FT erosion sensitivities under various vegetation coverage ranges.

TABLE 3 Sensitivity grades of FT erosion.

	Sensitivity				
	Insensitive	**Mild**	**Moderate**	**High**	**Extremely high**
Evaluation of estimate (S)	<2	2–3.5	3.5–5.5	5.5–7.5	≥7.5

TABLE 4 Statistics on the sensitivity of FT erosion.

Sensitivity	**Area (10^4 km^2)**	**A (%)**	**B (%)**
Insensitive	9.56	12.05	7.95
Mild	8.19	10.32	6.81
Moderate	42.29	53.27	35.16
High	18.74	23.60	15.57
Extremely high	0.61	0.77	0.51
Total of FT zone	79.40	100.00	66.00
Non-FT zone	40.90	—	34.00
Total	120.30	—	100.00

Note: A is the percentage of FT, zone area; and B is the percentage of total area.

TABLE 5 Weighting of FT erosion indictors.

Factor	**Annual range of temperature**	**Annual precipitation**	**Slope**	**Aspect**	**Vegetation coverage**
Weight	0.38	0.23	0.14	0.06	0.19

temporal resolution was 3 h. All images were resampled to a 90-m spatial resolution using the nearest sampling method.

The Moderate Resolution Imaging Spectroradiometer (MODIS) normalized difference vegetation index (NDVI) products (MOD13Q1 and MYD13Q1) were downloaded from NASA Earthdata Search (https://search.earthdata.nasa.gov/). The data are generated every 16 days at a 250-m spatial resolution. In this paper, MODIS products from 2016 to 2018 were used, and the spatial resolution was resampled to 90 m using the nearest sampling method.

The Climatic Research Unit (CRU) time-series (TS) v. 4.05 dataset comprises month-by-month variations in climate over the period 1901–2020 (Morice et al., 2012; Harris et al., 2020); from this dataset, we selected daily mean temperature as the variable. In addition, we selected surface temperature from the CMIP5 model (Taylor et al., 2012; Knutti and Sedláček, 2013). The CMIP5 contains four experiments: a historical experiment (1901–2018) and 3 future emission scenarios for 2006–2,100. In detail, the 3 future scenarios are the representative concentration pathways (RCPs) developed for the IPCC Fifth Assessment Report (AR5). The RCPs—originally RCP2.6, RCP4.5, and RCP8.5—are labeled after a possible range of radiative forcing values in the year 2,100 (2.6, 4.5, and 8.5 W/m^2, respectively). The details of the datasets used in this study are shown in Table 1.

Methods

Extraction of the freezing and thawing region

Qiu et al. (2000) indicated that the lower boundary of permafrost in the Tibetan Plateau is equivalent to the −2°C −−3°C isotherm of the annual average temperature. Hence, the −2.5°C isotherm of the annual average temperature was selected as the lower bound of the permafrost. The lower bound of the FT erosion area in Tibet was 200 m lower than the −2.5°C isotherm of the annual average temperature (Zhou et al., 2000; Zhang and Liu, 2005). Therefore, we assumed that the altitude of the −2.5°C isotherm minus 200 m was the lower bound of the FT erosion zone in Tibet. The altitude of the FT erosion lower bound was acquired according to Eq. 1:

$$H = \frac{66.3032 - 0.9197X_1 - 0.1438X_2 + 2.5}{0.005596} - 200 \quad (1)$$

where H is the altitude of the FT erosion lower bound, X_1 is the latitude (°) and X_2 is the longitude (°).

The freezing and thawing regions were extracted *via* the following: 1) extracting the latitude (X_1) layer and longitude (X_2) layer using the DEM; 2) calculating the altitude (H) and obtaining the potential FT erosion zone based on DEM values; and 3) removing the glacier area, lake area, and desertification area from the potential FT erosion area using a land cover type map.

Selection of evaluation factors

FT erosion is closely related to climate, topography, hydrology and vegetation (Guo et al., 2015). Zhang et al. (2007) summarized the natural factors that contribute to FT erosion: 1) temperature, including mean annual soil temperature and annual soil temperature range in FT erosion zone. 2) landform, which has an influence on the type and degree of erosion. 3) precipitation, which has an influence on the type and degree of erosion. 4) vegetation, which can mitigate some of the effects. 5) soil, FT erosion is closely related to the soil physical property. In this study, the selection of indicators was considered on the basis of empirical evidence from previous research (Shi et al., 2012; Guo et al., 2015; Lu et al., 2021). In addition, soil physical properties are often influenced by temperature, precipitation, and vegetation. Therefore, this paper selected five factors as the influencing factors of FT erosion, including the annual temperature range, annual precipitation, slope, aspect and vegetation coverage.

Temperature is an important criterion used to judge the FT state, which mostly occurs when the soil temperature fluctuates at approximately 0°C (Wang et al., 2007). The soil temperature changes periodically in the FT erosion zone with periodic changes in air temperature. Thus, the air temperature can be used as a substitute factor for soil temperature (Zhang et al., 2007; Shi et al., 2012). The air annual temperature range was calculated *via* a regression Eq. 2 among latitude, longitude and altitude as follows:

$$A = 3.1052 + 1.2418X_1 - 0.2275X_2 - 0.0004133X_3 \quad (2)$$

Where A is the annual temperature range, X_1 is the latitude, X_2 is the longitude, and X_3 is the altitude.

Precipitation is a driving force for material movement of erosion, and it increases the possibility of FT erosion. We obtained daily precipitation data (years: 2016–2018) by summing the 3-hourly precipitation. Then, the average annual precipitation was calculated by Eq. 3:

$$Y = \sum_{i=1}^{n} Y_i \quad (3)$$

Where n is the length of the time series of one year.

In addition, the slope affects the amount of FT erosion and the magnitude of erosion displacement. Aspect can lead to different types of FT erosion. Slope and aspect were extracted by the DEM using the slope and aspect tools in ArcGIS.

Vegetation plays an important role in suppressing the FT erosion process. Based on the maximum value of the MODIS NDVI in summer over the past three years (2016–2018) and the vegetation type map, the vegetation coverages of different

vegetation types were obtained by using the pixel dichotomy model:

$$f_g = \frac{NDVI - NDVI_{soil}}{NDVI_{veg} - NDVI_{soil}} \quad (4)$$

where f_g is the vegetation coverage and $NDVI_{soil}$ and $NDVI_{veg}$ are the NDVI values of the full soil coverage pixels and full vegetation pixels, respectively.

Sensitivity of the evaluation factors

The comprehensive evaluation of FT erosion represents a synthesis of multiple factors affecting this complex process of FT erosion (Xie et al., 2017). The evaluation is worked out based to the distribution situation of various factors values in Tibetan freeze-thaw zone. According to the specific distribution of each factor value in the FT erosion area of Tibet and based on the results of previous studies, the sensitivity levels of various factors affecting FT erosion were determined (Table 2). Figure 2 shows the sensitivity of each factor.

Evaluation factors that affect FT erosion were integrated to obtain a comprehensive evaluation index for the sensitivity assessment of FT erosion (Wang et al., 2004). The comprehensive evaluation index can be calculated by using Eq. 5:

$$S = \sqrt[n]{\prod_{i=0}^{n} C_i} \quad (5)$$

where S is the comprehensive evaluation factor, C_i is the grading assignment of factor I, and n is the number of factors. The sensitivity of FT erosion in the study area was then divided into five grades (Table 3).

Importance calculation of evaluation factors

In the previous studies, Analytic Hierarchy Process (AHP) method is widely used in the evaluation of FT erosion. Zhang et al. (2007) chose six factors to build the model for relative classification of FT erosion using AHP method. Hu et al. (2021) selected seven evaluation factors to analyze the temporal and spatial characteristics of FT erosion based on the AHP method. AHP is a qualitative and quantitative, systematic and hierarchical analysis method (Hu et al., 2021). The factors are grouped at different levels according to the correlation and subordination, and finally a multi-level analysis structure model is formed. Further, the AHP semi-quantitatively assigns the weight of each factor according to the subjective judgment of experts and the importance of factors, making the weight allocation more reasonable. In this study, we utilized AHP to reflect the effects of each factor on FT erosion. In details, the importance of each factor was obtained by constructing a decision model of 5 factors affecting FT erosion. The AHP model can be generally carried out according to the following steps:

(1) Build a judgment matrix. Pairwise comparison of each factor is used to evaluate the grade according to its importance, and a judgment matrix is formed according to the result of the pairwise comparison. The formula is:

$$a_{ij} = \frac{1}{a_{ji}} \quad (6)$$

Where i and j represent the different factor.

(2) consistency test. According to the judgment matrix, the weight value of each factor is calculated. In order to test whether the weight value is scientific, the consistency test of the judgment matrix is also required:

$$\lambda_{max} = \sum_{i=1}^{n} \frac{[A\omega]_i}{n\omega_i} \quad (7)$$

$$CI = \frac{\lambda - n}{n - 1} \quad (8)$$

$$CR = \frac{CI}{RI} \quad (9)$$

where λ_{max} is the largest eigenvalue; A refers to judgment matrix; ω is feature vector; n is the order of matrix; CI is the indicator of consistency; CR is test coefficient; RI is the mean random consistency.

Temperature stability

The coefficient of variation (CV) was employed to estimate temperature stability. The CV can be calculated as follows (Wang et al., 2004):

$$CV = \sigma/\mu \quad (10)$$

$$\sigma = \sqrt{\frac{1}{n}\sum_{i=1}^{n}(x_i - \mu)^2} \quad (11)$$

$$\mu = \frac{1}{n}\sum_{i=1}^{n} x_i \quad (12)$$

where σ represents the standard deviation of the annual air temperature; μ represents the average air temperature during the study period; n represents the number of years; and x_i represents the air temperature in the i*th* year.

A flow chart of evaluating the FT erosion sensitivity is shown as Figure 3, specifically as follows: 1) Data processing. 2) Comprehensive evaluation of FT erosion. 3) Prediction of future FT erosion sensitivity.

Results

Freeze-thaw erosion sensitivity

The distribution of FT erosion regions was extensive in Tibet (Table 4), with an area of 79.4×10^4 km^2 accounting for 66.00% of the total area, which indicated that FT erosion may be one of the main types of soil erosion. The area sensitive to FT erosion is 69.83×10^4 km^2, among which the moderate and more sensitive area is 61.64×10^4 km^2, accounting for 77.63% of the total FT erosion area in Tibet.

Significant differences were observed in the spatial distribution of FT erosion sensitivity in Tibet. The sensitivity map (Figure 4) shows that the sensitivity of FT erosion in southern high-altitude areas is higher than that in northern high-latitude areas. High-sensitivity areas and extremely high-sensitivity areas were mainly distributed in the southwest region. Some areas in the southeast were insensitive-sensitivity and mild-sensitivity because they were situated in mountain canyons.

The contribution of each factor to the FT erosion susceptibility is different, it is necessary to weight each influencing factor. According to the AHP method, the weight of factors was calculated by building a judgment matrix, and consistency check of result was done (Table 5). The judgment matrix constructed in this paper is a 5th-order matrix, and the maximum eigenvalue λ_{max} = 5.252, CI = 0.063. Finally, the test coefficient CR = 0.056 is obtained, which is less than 0.1, indicating that the judgment matrix has passed the consistency test, so the obtained weight values of each ecological evaluation factor are available.

Validation of Freeze–thaw erosion sensitivity results

We compared our results with regional soil erosion intensity product overlapped with the study area in the bulletin of soil and water conservation issued by the ministry of water resources of the People's Republic of China in 2019. One of the main reasons for using this product as comparison was that the erosion intensity was the most authoritative results of the official release. It was also convenient to make such a comparison because the product provided high-spatial resolution result over Shenza County. A comparation between our FT erosion sensitivity results and soil erosion intensity product is shown in Figure 5. It is worth noting that our sensitivity grading is different from the erosion intensity grading. Only five ratings of our sensitivity correspond to the top five ratings of erosion intensity. In general, FT erosion show consistent distribution and similar level, they gradually weakened from northeast to southwest. Therefore, FT erosion sensitivity result in this study is reliable, and have a good accuracy.

Erosion sensitivity response to temperature change

Among the necessary climatic conditions for the occurrence of freeze-thaw erosion, temperature is the most important influencing factor, with a weight value of 0.38 (Table 5). Figure 6A shows the extent of variability in relation to the mean of the air temperature from 2016 to 2018. Our calculated CV indicated that air temperature stability is lower in western Tibet than in eastern Tibet, and the highest CV is located in northwestern Tibet, which means that the air temperature stability is lowest in the northwest. Figure 6B shows the mean CV in Tibet under different sensitivities, indicating that the CV has a high correlation with FT erosion sensitivity.

Prediction of future Freeze-thaw erosion sensitivity

In this study, we evaluated the agreement between CMIP5 air temperature anomalies and CRU observations. We took the average of the three CMIP5 scenarios as the air temperature. The correlation coefficient, RMSE and MAE were 0.70, 0.45°C, and 0.35°C, respectively. To further evaluate the agreement between the averaged CMIP5 air temperature and CRU observations in Tibet, we compared the time series and trends in annual temperatures (Figure 7). The time series of MAT (mean annual air temperature) showed increasing temperatures during 1901–2018 for the air temperatures from CMIP5 models and CRU observations. The MAT from CRU observations increased significantly at a rate of 0.079°C decade^{-1}, while the MAT trends from CMIP5 increased at a rate of 0.125°C decade^{-1}. The MAT time-series anomalies were very similar to those from CRU and CIMP5 for Tibet. This similarity indicated that CMIP5 scenarios correlate well with CRU and that the average MAT was increasingly warmer.

Figure 8 shows the trend of the overall annual average temperature in Tibet from 2019 to 2,100. The RCP2.6 scenario presented a decrease at a rate of 0.03°C decade^{-1} (p<0.05), the RCP4.5 scenario exhibited an increase at a rate of 0.202°C decade^{-1} (p<0.05), and the RCP8.5 scenario increased significantly at a rate of 0.488°C decade^{-1} (p<0.05). Both RCP 4.5 and RCP 8.5 between 2019 and 2,100 showed an obvious warming trend in temperature throughout this century, and only RCP 2.6 did not show a general increase with time. In addition, basing on the CVs of every three years, we analyzed the CV changes in Tibet over the next 30 years under different scenario models. As shown in Figure 8, the CV of RCP8.5 scenario has more significant volatility compared with

RCP2.6 and RCP4.5. It indicated that RCP8.5 scenario is more prone to FT erosion than RCP2.6 and RCP4.5, in the future.

To better understand the spatial and temporal variation characteristics of CV in Tibet, the air temperatures from CMIP5 under three scenarios were used to calculate the spatial distribution of CV from 2019 to 2,100. The mean CVs in RCP 2.6, 4.5 ,and 8.5 were 0.0020, 0.0023 and 0.0038 over Tibet, respectively. The distribution of CV varied greatly for different scenarios (Figure 9). The CVs of the three scenarios in central and western Tibet were higher than those in eastern Tibet, which means that midwestern Tibet is more prone to FT erosion.

Discussion

FT erosion is a soil erosion phenomenon in permafrost regions and represents the main type of soil erosion in alpine regions. FT erosion causes serious harm to farmlands, grasslands, roads and railways and is widespread in Tibet. Thus, evaluating the sensitivity of FT erosion is important. In this study, the sensitivity of FT erosion was obtained by comprehensively evaluating the temperature, precipitation, slope, aspect and vegetation coverage. To further explore the influence of each factor on FT erosion, the FT erosion under each factor condition was analyzed individually.

The influence of the annual temperature range on Freeze-thaw erosion

Figure 10 shows the sensitive area ratios (proportion of different degrees of FT erosion in the total FT area) of annual temperature in five ranges (≤18°C, 18–20°C, 20–22°C, 22–24°C ,and >24°C). High- and extremely high-sensitivity areas were mainly in the temperature range of >18°C, accounting for more than 25% of the FT erosion area. Extremely high-sensitivity areas occurred only in the temperature belt of >20°C, and the FT erosion area occupied by each temperature belt was less than 2%. With increases in the temperature difference, the FT process increases; additionally, with increases in the frozen layer and melted layer depths, the degree of FT erosion will become more severe.

The influence of annual precipitation on Freeze-thaw erosion

Precipitation, consisting of rainfall and snowfall, affects the intensity of FT erosion. Water content affects the stability of soil aggregates when soil is frozen (Lehrsch et al., 1991), and precipitation is an important source of soil water content that directly changes the soil content. Figure 11 shows the FT erosion area ratios under different precipitation levels of ≤100 mm, 100 mm–200 mm, 200 mm–300 mm, 300 mm–400 mm, and 400 mm–500 mm. Extremely high sensitivity occurred only in areas with precipitation greater than 100 mm. When the precipitation reached 600 mm, the proportions of high and extremely high sensitivities tended to be stable as precipitation increased because vegetation began to flourish, which effectively reduced the sensitivity of FT erosion.

The influence of slope and aspect on Freeze-thaw erosion

The sensitive area ratios for different slope ranges of 0–3, 3–8, 8–15, 15–25, and >25 are shown in Figure 12. With increasing slope, the FT erosion degree showed an increasing trend. Insensitive FT erosion was mainly concentrated in the 0–3 slope belt, which accounted for 34% of the FT area. High and extremely high values mainly occurred in areas with slopes greater than 3, which accounted for more than 20% of the FT area, and in areas with high and extremely high sensitivity at a slope >15. Intense and extremely high erosion dominated the areas where the slope was >25, compared with the other slope belts. To reduce the possibility of FT erosion, we must strengthen the restoration and improvement of sloping lands and cultivated land.

Figure 13 shows the FT erosion area ratios under the different aspect ranges of 0–45°/315°–360°, 45°–135°, 135°–225°, and 225°–315°. The outer ring represents four slope directions: sunny slope, semi-sunny slope, semi-shady slope, and shady slope. The inner ring indicates the sensitivity ratio of each slope direction. The ratio directly indicates the sensitivity of FT erosion to the four aspects. Among all aspects, sunny slopes had the largest ratio of high and extremely high sensitivities (with a ratio of 43.6%). In addition, the FT erosion on sunny slopes and semi-shady slopes was more serious than that on shady slopes and semi-shady slopes. The absorbed solar radiation difference between different slopes (sunny slope and shady slope) resulted in thermal differences (Chou et al., 2010; Pei et al., 2017), and the soil's temperature difference on sunny slopes was greater than that on shady slopes. The change in the temperature difference led to more serious erosion on the sunny slope than on the shady slope. In addition, the difference between the semi-sunny slope and sunny slope decreased gradually with increasing elevation; thus, erosion on the semi-sunny slope was more serious than that on shady and semi-shady slopes.

The influence of vegetation coverage on Freeze-thaw erosion

Vegetation not only improves the soil stability but also reduces the soil temperature range. Therefore, vegetation can effectively reduce the sensitivity of soil to FT erosion (Bargiel et al., 2013). Unique terrestrial ecosystems and atmospheric conditions have contributed to the development of diverse biomes and

characteristic altitudinal distribution patterns of vegetation in Tibet (Luo et al., 2002), which extend from subalpine coniferous forest to alpine desert (Figure 14). The influence of vegetation on FT erosion is obvious, as shown in Figure 15, as larger vegetation coverage corresponds to milder FT erosion action. In particular, when vegetation coverage was <20, high and extremely high sensitivities accounted for 27%. Different vegetation types play different roles in mitigating FT erosion. For instance, the ratios of extremely high probability in the alpine desert and alpine desert steppe were larger than others due to weaker mitigation (Figure 15). FT erosion was slight in mountain evergreen broad-leaved forest, where dense vegetation effectively protected the soil from erosion.

Conclusion

The main goal of this research was to assess FT erosion sensitivity and evaluate the distribution of FT erosion probability in Tibet. Five factors were selecteded, and we explored the influence of each factor individually on FT erosion. Specifically, the conclusions of this paper are as follows:

(1) The area sensitive to FT erosion covered 69.83 km^2×104 km^2, with the moderately and more sensitive areas covering 61.64 km^2×104 km^2 in Tibet.
(2) Moderate-sensitivity types were distributed in the alpine arid regions, and high and extremely high sensitivity were mainly distributed in alpine desert and alpine desert steppe areas.
(3) Annual temperature range, slope and aspect accelerate soil FT erosion. Vegetation coverage inhibit FT erosion. The proper increase of precipitation strengthened the role of vegetation. Under the comprehensive action of various factors, the melting of frozen layer in Tibet have accelerated the soil FT erosion.
(4) In the future, midwestern Tibet will be more prone to FT erosion than other areas.

Data availability statement

The original contributions presented in the study are included in the article/supplementary material, further inquiries can be directed to the corresponding author.

Author contributions

All authors listed have made a substantial, direct, and intellectual contribution to the work and approved it for publication.

Funding

This research was funded by the second Tibetan Plateau Scientific Expedition and Research Program (STEP), Grant No. 2019QZKK0603.

Conflict of interest

The authors declare that the research was conducted in the absence of any commercial or financial relationships that could be construed as a potential conflict of interest.

Publisher's note

All claims expressed in this article are solely those of the authors and do not necessarily represent those of their affiliated organizations, or those of the publisher, the editors and the reviewers. Any product that may be evaluated in this article, or claim that may be made by its manufacturer, is not guaranteed or endorsed by the publisher.

References

Bargiel, D., Herrmann, S., and Jadczyszyn, J. (2013). Using high-resolution radar images to determine vegetation cover for soil erosion assessments. *J. Environ. Manag.* 124, 82–90. doi:10.1016/j.jenvman.2013.03.049

Chou, Y., Sheng, Y., Li, Y., Wei, Z., Zhu, Y., and Li, J. (2010). Sunny–shady slope effect on the thermal and deformation stability of the highway embankment in warm permafrost regions. *Cold Regions Sci. Technol.* 63 (1), 78–86. doi:10.1016/j.coldregions.2010.05.001

Dong, R., Xu, Z., and Yang, Y. (2000). *Freeze-thaw erosion in qinghai-tibet plateau*. River: Yangtze, 39–41.

Eigenbrod, K. D. (1996). Effects of cyclic freezing and thawing on volume changes and permeabilities of soft fine-gained soils. *Can. Geotech. J.* 33 (4), 529–537. doi:10.1139/t96-079-301

Falorni, G., Teles, V., Vivoni, E. R., Bras, R. L., and Amaratunga, K. S. (2005). Analysis and characterization of the vertical accuracy of digital elevation models from the Shuttle Radar Topography Mission. *J. Geophys. Res.* 110 (2), F02005. doi:10.1029/2003jf000113

Ferrick, M. G., and Gatto, L. W. (2005). Quantifying the effect of a freeze–thaw cycle on soil erosion: Laboratory experiments. *Earth Surf. Process. Landf.* 30 (10), 1305–1326. doi:10.1002/esp.1209

Field, C. B., Barros, V. R., Mastrandrea, M. D., Mach, K. J., Abdrabo, M. K., Adger, N., et al. (2014). "Summary for policymakers," in *Climate change 2014: impacts, adaptation, and vulnerability. Part A: global and sectoral aspects. Contribution of Working Group II to the Fifth Assessment Report of the Intergovernmental Panel on Climate Change*. (Cambridge University Press), 1–32.

Gao, H., Zhang, W., and Chen, H. (2018). An improved algorithm for discriminating soil freezing and thawing using AMSR-E and AMSR2 soil moisture products. *Remote Sens.* 10 (11), 1697. doi:10.3390/rs10111697

Guo, B., and Jiang, L. (2017). Evaluation of freezing-thawing erosion intensity in qinghai-tibet plateau based on multi-source space-coupled data. *Bull. Soil Water Conserv.* 37, 12–19. doi:10.1080/19475705.2018.1564705

Guo, B., Zhang, F., Yang, G., and Jiang, L. (2017). Improved method of freeze–thaw erosion for the three-river source region in the qinghai–Tibetan plateau, China. *Geomatics, Nat. Hazards Risk* 8 (2), 1678–1694. doi:10.1080/19475705.2017.1370026

Guo, B., Zhou, Y., Zhu, J., Liu, W., Wang, F., Wang, L., et al. (2015). An estimation method of soil freeze-thaw erosion in the Qinghai–Tibet Plateau. *Nat. Hazards (Dordr).* 78 (3), 1843–1857. doi:10.1007/s11069-015-1808-5

Harris, I., Osborn, T. J., Jones, P., and Lister, D. (2020). Version 4 of the CRU TS monthly high-resolution gridded multivariate climate dataset. *Sci. Data* 7 (1), 109. doi:10.1038/s41597-020-0453-3

Hu, T., Fan, J., Yu, X., Zhou, Y., Zhang, P., and Han, L. (2019). Evaluation of freeze–thaw erosion in tibet based on cloud model. *Front. Earth Sci.* 15, 495. doi:10.20944/preprints201909.0201.v1

Huffman, G. J., Adler, R. F., Bolvin, D. T., and Nelkin, E. J. (2010). "The TRMM multi-satellite precipitation analysis (TMPA)," in *Satellite rainfall applications for surface hydrology* (Springer), 3–22.

Knutti, R., and Sedláček, J. (2013). Robustness and uncertainties in the new CMIP5 climate model projections. *Nat. Clim. Chang.* 3 (4), 369–373. doi:10.1038/nclimate1716

Kong, B., and Yu, H. (2013). Estimation model of soil freeze-thaw erosion in silingco watershed wetland of northern tibet. *Sci. World J.* 2013, e636521–7. doi:10.1155/2013/636521

Lehrsch, G. A., Sojka, R. E., Carter, D. L., and Jolley, P. M. (1991). Freezing effects on aggregate stability affected by texture, mineralogy, and organic matter. *Soil Sci. Soc. Am. J.* 55, 1401–1406. doi:10.2136/sssaj1991.03615995005500050033x

Li, D., Wei, X., Li, X., and Li, Y. (2015). Sensitivity evaluation of freeze-thaw erosion in Gansu province based one RS and GIS. *Res. Soil Water Conservation* 22, 1–6. doi:10.13869/j.cnki.rswc.2015.02.002

Li, H., Liu, S., Zhong, X., Zhang, J., and Wang, X. (2005). GIS-based sensitivity evaluation on freeze-thaw erosion in Tibet. *Soil Water Conservation China* 7, 44–46. doi:10.14123/j.cnki.swcc.2005.07.024

Li, S., Lai, Y., Pei, W., Zhang, S., and Zhong, H. (2014). Moisture–temperature changes and freeze–thaw hazards on a canal in seasonally frozen regions. *Nat. Hazards (Dordr).* 72 (2), 287–308. doi:10.1007/s11069-013-1021-3

Li, Z., Zhu, B., and Li, P. (2008). Advancement in study on soil erosion and soil and water conservation. *Actor Pedol. Sinaica* 45, 802–809. doi:10.3232/SJSS.2014.V4.N3.05

Liu, S., Liu, B., Tao, H., and Zhang, L. (2013). The current situation and countermeasures of freeze-thawing erosion in China. *Soil Water Conserv. China* 10, 41–44. doi:10.14123/j.cnki.swcc.2013.10.012

Liu, S., Zhang, J., and Gu, S. (2006). Study on the soil erosion types in Tibet. *J. Mt. Sci.* 24, 592–596. doi:10.3969/j.issn.1008-2786.2006.05.013

Lu, Y., Liu, C., Ge, Y., Hu, Y., Wen, Q., Fu, Z., et al. (2021). Spatiotemporal characteristics of freeze-thawing erosion in the source regions of the chin-sha, ya-lung and Lantsang rivers on the basis of GIS. *Remote Sens.* 13 (2), 309. doi:10.3390/rs13020309

Luo, T., Li, W., and Zhu, H. (2002). Estimated biomass and productivity of natural vegetation on the Tibetan plateau. *Ecol. Appl.* 12 (4), 980–997. doi:10.1890/1051-0761(2002)012[0980:EBAPON]2.0.CO;2

Morice, C. P., Kennedy, J. J., Rayner, N. A., and Jones, P. D. (2012). Quantifying uncertainties in global and regional temperature change using an ensemble of observational estimates: The HadCRUT4 data set. *J. Geophys. Res.* 117 (8). doi:10.1029/2011jd017187

Pei, W., Zhang, M., Li, S., Lai, Y., Jin, L., Zhai, W., et al. (2017). Geotemperature control performance of two-phase closed thermosyphons in the shady and sunny slopes of an embankment in a permafrost region. *Appl. Therm. Eng.* 112, 986–998. doi:10.1016/j.applthermaleng.2016.10.143

Qiu, G., Zhou, Y., and Cheng, G. (2000). *Geocryology in China*. Beijing: Science Press.

Reichstein, M., Bahn, M., Ciais, P., Frank, D., Mahecha, M. D., Seneviratne, S. I., et al. (2013). Climate extremes and the carbon cycle. *Nature* 500 (7462), 287–295. doi:10.1038/nature12350

Shi, Z., Tao, H., Liu, S., Liu, B., and Guo, B. (2012). Evaluation and analysis of freeze-thawing erosion in sanjiangyuan area based on GIS. *Trans. Chin. Soc. Agric. Eng.* 28, 214–221. doi:10.1007/s11707-021-0873-1

Taylor, K. E., Stouffer, R. J., and Meehl, G. A. (2012). An overview of CMIP5 and the experiment design. *Bull. Am. Meteorological Soc.* 93 (4), 485–498. doi:10.1175/bams-d-11-00094.1

Teng, H., Liang, Z., Chen, S., Liu, Y., Viscarra Rossel, R. A., Chappell, A., et al. (2018). Current and future assessments of soil erosion by water on the Tibetan Plateau based on RUSLE and CMIP5 climate models. *Sci. Total Environ.* 635, 673–686. doi:10.1016/j.scitotenv.2018.04.146

Wang, D., Ma, W., Niu, Y., Chang, X., and Wen, Z. (2007). Effects of cyclic freezing and thawing on mechanical properties of Qinghai–Tibet clay. *Cold Regions Sci. Technol.* 48 (1), 34–43. doi:10.1016/j.coldregions.2006.09.008

Wang, L. Y., Xiao, Y., Jiang, L., and Ouyang, Z. Y. (2017). Assessment and analysis of the freeze-thaw erosion sensitivity on the Tibetan Plateau. *J. Glaciol. Geocryol.* 39 (1), 61–69. doi:10.7522/j.issn.1000-0240.2017.0008

Wang, T., Yang, D., Yang, Y., Piao, S., Li, X., Cheng, G., et al. (2020). Permafrost thawing puts the frozen carbon at risk over the Tibetan Plateau. *Sci. Adv.* 6 (19), eaaz3513. eaaz3513. doi:10.1126/sciadv.aaz3513

Wang, X., Zhong, X., and Fan, J. (2004). Assessment and spatial distribution of sensitivity of soil erosion in Tibet. *J. Geogr. Sci.* 14 (1), 41–46. doi:10.1007/BF02873089

Wei, X., Ding, Y., and Li, X. (2012). Review and prospect of freeze-thawing-induced erosion research. *Res. Soil Water Conserv.* 19, 271–275.

Xie, S., Qu, J., Xu, X., and Pang, Y. (2017). Interactions between freeze–thaw actions, wind erosion desertification, and permafrost in the Qinghai–Tibet Plateau. *Nat. Hazards (Dordr).* 85 (2), 829–850. doi:10.1007/s11069-016-2606-4

Zhang, J., and Liu, S. (2005). A new method to define the distribution of freeze-thawing erosion areas in Tibet. *Geogr. Geo-Inf. Sci.* 21, 32–34.

Zhang, J., Liu, S., and Yang, S. (2007). The classification and assessment of freeze-thaw erosion in Tibet. *J. Geogr. Sci.* 17 (2), 165–174. doi:10.1007/s11442-007-0165-z

Zhang, K., and Liu, H. (2018). Research progress and prospect of freeze-thaw erosion in black soil areas in northeast China. *Sci. Soil Water Conserv.* 16, 17–24. doi:10.16843/j.sswc.2018.01.003

Zhang, R., Wang, X., Fan, H., Zhou, L., Wu, M., and Liu, Y. (2009). Study on the zonal erosion characteristics of freezing-thawing zone in China. *Sci. Soil Water Conserv.* 7, 24–28. doi:10.1051/e3sconf/202123701026

Zhou, Y., Guo, D., Qiu, G., Cheng, G., and Li, S. (2000). *Geocryology in China*. 1st ed. Beijing, China: Science Press, 15–115.